Numerical Modelling and Bearing Capacity Analysis of Pile Foundation

4 authors:

Kazimierz Józefiak
Warsaw University of Technology
26 PUBLICATIONS   **90** CITATIONS

Artur Zbiciak
Warsaw University of Technology
169 PUBLICATIONS   **631** CITATIONS

Maciej Maślakowski
Warsaw University of Technology
21 PUBLICATIONS   **156** CITATIONS

Tomasz Piotrowski
Warsaw University of Technology
52 PUBLICATIONS   **452** CITATIONS

Some of the authors of this publication are also working on these related projects:

Polymer waste aggregates in concrete, polymer concrete and polymer-cement concrete View project

New Generation Shielding Concrete against ionizing radiation View project

XXIV R-S-P seminar, Theoretical Foundation of Civil Engineering (24RSP) (TFoCE 2015)

Numerical modelling and bearing capacity analysis of pile foundation

Kazimierz Józefiak[a],*, Artur Zbiciak[a], Maciej Maślakowski[a], Tomasz Piotrowski[b]

[a]Warsaw University of Technology, Institute of Roads and Bridges, 16 Armii Ludowej Ave., 00-637 Warsaw, Poland
[b]Warsaw University of Technology, Institute of Building Engineering, 16 Armii Ludowej Ave., 00-637 Warsaw, Poland

Abstract

The problem of designing deep foundations is related to many civil engineering structures as it is becoming more common and frequent to construct buildings on soft soils. Pile foundation is a popular deep foundation type used to transfer superstructure load into subsoil and bearing layers. However, accurate prediction of piles' settlement is particularly difficult concerning complicated consolidation process and pile-soil interaction. The objective of this paper is to model a soil-pile system using FEM implemented in Abaqus software. The numerical results of pile bearing capacity and pile settlement were compared with static load test results of CFA piles carried out during construction of Łazienkowska tract flyovers in Warsaw and with engineering analytical calculations according to Eurocode 7 and Polish Standard Code.

1. Introduction

Piles are commonly used to transfer superstructure load into subsoil and a stiff bearing layer. As it was emphasized by Lambe and Whitman [1], a pile foundation, even in the case of single pile, is statically indeterminate to a very high degree. The proper solution to a given pile foundation problem requires empirical knowledge and the results of pile tests at the actual site.

----

* Corresponding author. Tel.: +48-22-825-59-37; fax: +48-22-825-88-99.
   E-mail address: k.jozefiak@il.pw.edu.pl

The main goal of this paper is to present a model of the soil-pile system using FEM implemented in Abaqus software. Some theoretical problems arising from constitutive models of soils to be applied are also pointed out. The numerical results of pile bearing capacity and pile settlement were compared with static load test results of CFA piles carried out during construction of Łazienkowska tract flyovers in Warsaw and with engineering analytical calculations according to Eurocode 7 and Polish Standard Code.

2. Matching MC and EDP parameters

Assuming $0 \geq \sigma_1 \geq \sigma_2 \geq \sigma_3$, for triaxial compression $\sigma_1 = \sigma_2 \geq \sigma_3$ and for extension $\sigma_1 \geq \sigma_2 = \sigma_3$. Linear extended Drucker-Prager (EDP) yield surface can then be expressed for triaxial compression as

$$(\sigma_1 - \sigma_3) + \frac{\tan \beta}{2 + \frac{1}{3}\tan \beta}(\sigma_1 + \sigma_3) - \frac{2d}{2 + \frac{1}{3}\tan \beta} = 0 \tag{1}$$

and for triaxial tension as

$$(\sigma_1 - \sigma_3) + \frac{\tan \beta}{\frac{2}{K} - \frac{1}{3}\tan \beta}(\sigma_1 + \sigma_3) - \frac{2d}{\frac{2}{K} - \frac{1}{3}\tan \beta} = 0 \tag{2}$$

In order to obtain the same yield surface for triaxial compression and tension conditions, one needs to set (see Equations (1) and (2))

$$K = \frac{1}{1 + \frac{1}{3}\tan \beta} \tag{3}$$

Condition (3) means that regardless of triaxial test conducted, the resulting yield surface is the same.
The MC yield surface is as follows:

$$\sigma_1 - \sigma_3 + (\sigma_1 + \sigma_3)\sin \phi - 2c\cos \phi = 0 \tag{4}$$

From comparison of Eq. (1) and (4) the well-known equations are obtained which match MC and EDP parameters in triaxial conditions

$$\tan \beta = \frac{6\sin \phi}{3 - \sin \phi} \quad ; \quad d = \frac{6\cos \phi}{3 - \sin \phi}c \tag{5}$$

From Eq. (3), using (5) we can see that

$$K = \frac{3 - \sin \phi}{3 + \sin \phi} \tag{6}$$

However $K \geq 0.778$ is needed for the EDP surface to remain convex. Therefore this procedure of matching MC and EDP models in deviatoric plane is possible only for $\phi \leq 22°$. In the case of sand for which $\phi \approx 30°$ the authors assumed *K=0.778* for EDP model and β calculated from Eq. (5).
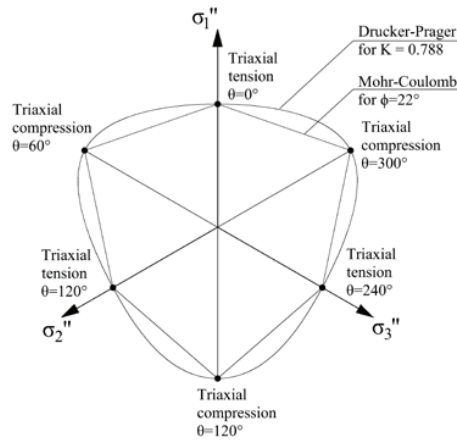
Fig. 1. Mohr-Coulomb and Extended Drucker-Prager models match in deviatoric plane for triaxial conditions.

Triaxial tension and compression conditions can be described using Lode's angle [2] which can be expressed using deviator stress invariants

$$\cos 3\theta = \frac{3\sqrt{3}}{2} \frac{\det(\mathbf{s})}{(\frac{1}{2}\mathbf{s}\cdot\mathbf{s})^{3/2}} \tag{7}$$

Assuming $0 \geq \sigma_1 \geq \sigma_2 \geq \sigma_3$ for triaxial compression we get $\cos 3\theta = -1$ which gives $\theta = \frac{1}{3}(\pi + 2\pi \cdot n)$. For triaxial tension $\theta = \frac{2}{3}\pi \cdot n$. These values of Lode's angle indicate where MC and EDP yield surfaces intersect each other in deviatoric plane for $\phi \leq 22°$ as shown in Figure 1. For $\phi > 22°$ the surfaces doesn't intersect at triaxial tension points.

3. FEM pile model compering with field loading test

3.1. Pile test loading

A pile load test consists of the static load increments application to a test pile and measuring the deflection of the pile. A static pile test can be conducted both in order to indicate for the contractor the type of driving conditions as well as to convince the building authorities that the pile is adequate to support the design load [1].

Loading tests provide the most reliable results of pile capacity. Detailed load test procedures are described in relevant codes [3, 4]. For the pile analyzed here test loading shown in Figure 2 gave pile settlement response shown in Figure 4 [5]. For this particular pile it could be seen from test results that pile bearing capacity wasn't achieved and bearing capacity was assumed to be equal to maximum applied load Q_{max}=1108 kN. Q_{max} induced settlement equal to 4.62 mm.

3.2. FEA of pile settlement

Geometry of the analyzed pile and geotechnical conditions are shown in Figure 3a. Finite element method calculations were carried out using Abaqus commercial software. The problem was solved as axisymmetric. FEM model, representing half of a cross-section, was assumed to be 25.0 meters wide and 20.0 meters high. Such dimensions were estimated by solving the problem for linear-elastic material model and examining stress and strain response range.
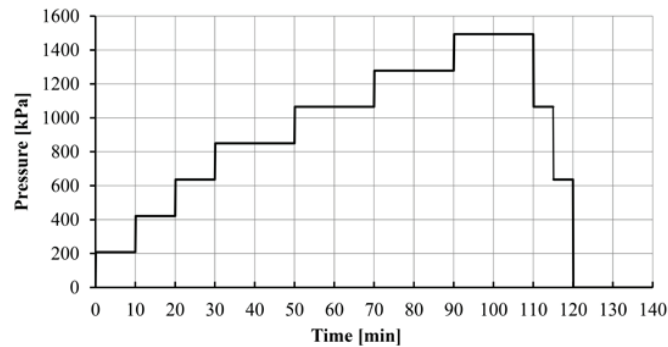
Fig. 2. Pressure amplitude applied to pile's top during field test and FEA.

Table 1. Material parameters of soil

Soil layer	Elasticity		Mohr - Coulomb			Extended Drucker-Prager				General properties		
	E	v	ϕ'	c'	ψ	β'	d'	K	ψ	ρ_d	e	k
	[kPa]	[-]	[°]	[kPa]	[°]	[°]	[kPa]	[-]	[°]	[kg/m³]	[-]	[m/min]
Embankment (Sand/Gravel)	55000	0.25	30	≈0	2	52	≈0	0.778	2	1526	0.74	0.06
Medium Sand	80000	0.25	32	≈0	2	50	≈0	0.778	2	1606	0.65	0.06

Initial conditions were applied for effective overburden stress, void ratio and pore water pressure. The coefficients of horizontal earth pressure at rest were calculated as $K_o = (1 - \sin\phi)$. Boundary conditions were as follows: vertical displacement constrained at the bottom of the model, horizontal displacement constrained at the far vertical edge, pore pressure constrained to be zero at the water table level (-6.5 m). Gravitational force was applied to the whole model. Load amplitude shown in Figure 2 was applied to the upper tip of the pile. This loading was the same as the loading cycle of the field loading test.

In case of the road construction analyzed herein, no specialized geotechnical tests were conducted except for drillings and dynamic probing field test which provided relative density (I_D) values. In fact this is often the case. That implied using simple constitutive models of geomaterials like Mohr-Coulomb and Extended Drucker-Prager.

Using Polish Standard Code [3] it was possible to estimate linear elasticity and Coulomb-Mohr yield criterion parameters basing on I_D values and soils' types. Material parameters of the two soil layers are shown in Table 1 and Figure 3. Permeability was assumed according to [6] for medium sand. Drucker-Prager parameters were calculated according to this paper's previous section considerations. The reinforced concrete pile was modelled as linear elastic with $E = 31.1\,\text{GPa}$, $v = 0.2$ and $\rho = 2400 kg/m^3$.

Dry soil conditions were assumed above the water table. Such assumption could be made because capillary zone in sands is small. Therefore, stress-only axisymmetric 8-node biquadratic quadrilateral finite elements without reduced integration were applied within the water table. Fully saturated flow was assumed under the water table level and for this region, 8-node pore fluid/stress axisymmetric quadrilateral elements without reduced integration were applied with biquadratic displacement and bilinear pore pressure interpolation. The whole model was discretized into 9796 finite elements with 30076 nodes. The mesh is shown in Fig. 3b.

Interaction between the pile and soil was modelled using simple Coulomb friction model where friction coefficient was an input parameter and can be defined as
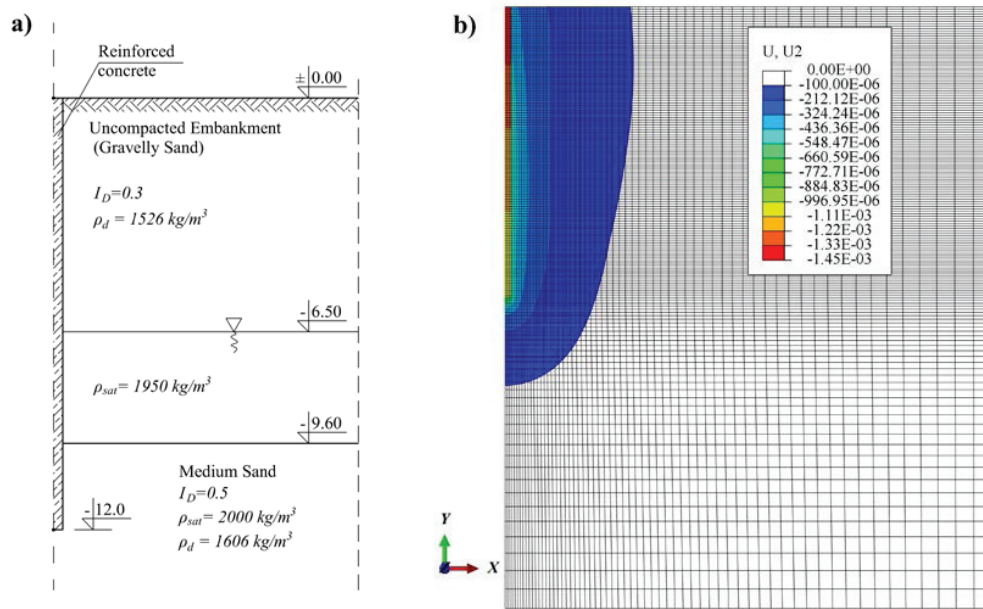
$$\mu = \tan\delta \tag{8}$$

Fig. 3. (a) Model's geotechnical conditions; (b) Mesh and vertical displacement contours at $t = 110$ min.

where δ is interface frictional angle. Here $\delta = \phi'$ was assumed as suggested by Kuhlawy [3] see next section of this paper). A penalty-type, stiffness method was used in Abaqus for imposing frictional constraints. This method permits some relative motion of the surfaces (an "elastic slip") when contact surfaces should be sticking It is computationally efficient and provides generally accurate results.

In case of the second modelling approach contact conditions with relative motion being constrained were assumed (pile and soil nodes were "tied"). In order to check elastic slip influence, the authors also performed analysis using penalty contact enforcement method with $\mu = \infty$.

The analysis was conducted in 3 steps. The first step was a geostatic-type step used to verify that the initial geostatic stress field is in equilibrium with applied loads and boundary conditions. Load amplitude was applied during the next two coupled pore fluid flow and stress steps, as different calculation increments were needed for loading and unloading parts of the amplitude. Automatic stabilization procedure was used in Abaqus to deal with local instabilities related to plastic flow.

Several calculations were carried out using different constitutive models and soil-pile interface definitions. Comparison between different FEA approaches and loading test results is shown in Fig. 4. Fig. 3b shows contour plot of vertical displacements around the pile at the end of the loading stage.

4. Bearing capacity analysis of piles in sand

4.1. Analytical estimation of pile bearing capacity

There are two routinely used methods of piles' bearing capacity calculation: total stress approach (α-method) and effective stress approach (β-method). An outline of these methods and problems related to them can be found e. g. in [7, 8]. Total capacity of a single pile is estimated as follows:
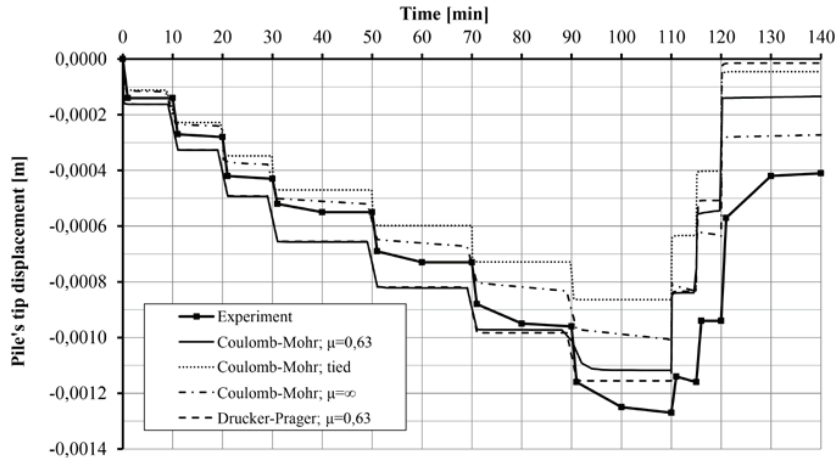
$$P_u = Q_b + Q_f = q_b A_b + \tau_s A_s$$

(9)

Fig. 4. Comparison of FEA and pile test loading results

where P_u – total ultimate capacity, q_b – pressure on pile base, τ_s – friction along pile shaft, A_b – section area of the pile base, A_s – area of the pile shaft. In case of piles constructed within sand layer, analyzed in this paper, effective stress approach is appropriate and the unit shaft resistance is calculated as:

$$\tau_s = \beta\sigma'_{vs} \tag{10}$$

where σ'_{vs} denotes effective overburden pressure and

$$\beta = K\tan\delta \tag{11}$$

where δ is interface frictional angle and K is lateral earth pressure coefficient related to the lateral earth pressure coefficient at rest $K_0 = (1-\sin\phi)$. Kuhlawy [9] and Reese and O'Neill [10], for example, recommend values of K/K_0 taking into account pile displacement and construction methods. For drilled shaft cast-in-place K/K_0 ranges between 2/3 and 1.0. The angle of friction between the pile shaft and the soil, δ, depends on construction method as well, being a function of pile surface roughness, and can be related to effective friction angle ϕ'. Here the authors assumed $\delta = \phi'$ as it was done previously in the FEM analysis. The value is recommended by Kuhlawy [9] for rough concrete, cast-in-place. On the other hand Polish Standard Code [3] suggests $\delta = \frac{2}{3}\phi'$ for rough concrete retaining walls.

McClelland [11] suggests values of β for sands ranging from 0.15 to 0.35. Here, for the uncompacted embankment layer $\beta^{UE} = \frac{2}{3}K_0\tan\phi' = 0.192$ and for the medium sand layer $\beta^{MSa} = \frac{2}{3}K_0\tan\phi' = 0.196$ which was within the range.

For a pile embedded in a layered system containing *n* layers Q_f has to be calculated as follows:

$$Q_f = \sum_{i=1}^{n}[\beta_i(\sigma_{vs})_i \cdot (A_s)_i] \tag{12}$$

For the analyzed pile, $Q_f = 307kN$ was obtained.

The end-bearing stress for sands is estimated as

$$q_b = N_q\sigma'_{vb} \tag{13}$$

where N_q – bearing capacity factor, σ'_{vb} – effective overburden pressure at the pile base. There are several ways of calculating N_q coefficient, assuming limited σ'_{vb} ($\sigma'_{vb} = \gamma' z_c$ under critical depth z_c) or unlimited values of σ'_{vb} [7, 12].

Berezantzev et al. [13], for example, deduced a graph relating N_q to ϕ' assuming limited σ'_{vb}. From this graph, for $\phi' = 32°$, $N_q \cong 40$ with z_c depending on pile's diameter and construction method.

Janbu [14] proposed a relationship

$$N_q = \left(\tan\phi' + \sqrt{1 + \tan^2\phi'} \right)^2 \text{Exp}(2\eta \tan\phi') \tag{14}$$

where η – is an angle defining the shape of the shear surface around the tip of a pile. This coefficient ranges from $\pi/3$ for soft clays to 0.58π for dense sands.

Relationship (14), for $\eta = \pi/2$, gave $N_q = 23$. For farther calculations the authors assumed this value and unlimited σ'_{vb}. That gave $q_b = 3445 kPa$ and $Q_b = 698 kN$.

Polish Standard Code gives tabularized maximum values of q_s and q_b depending on relative density I_D and soil's type. q_b is assumed to linearly change with depth to a critical depth z_c from which it becomes constant (limited σ'_{vb}). Calculations according to the code yield $Q_b^{PSC} = 546 kN$ and $Q_s^{PSC} = 764 kN$. Comparison of two different analytical approaches and test loading is shown in Figure 5.

4.2. FEA of bearing capacity

Finite element model described in section 3 was used to perform bearing capacity calculations. The problem was run in 2 steps. During the first step geostatic equilibrium was achieved. In step 2, coupled analysis was invoked and the pile displacement was applied using the vertical speed boundary condition to force the top surface to move 0.01 m/min. The pile was constructed in sand so relatively high speed could be used to achieve drained conditions. Excess pore water pressure rise under the pile was recorded to confirm drainage. For Extended Drucker-Prager model associated flow had to be assumed ($\psi \approx \beta$) to deal with convergence problems. The pile load versus settlement curve obtained from the FEA is shown in Figure 5.
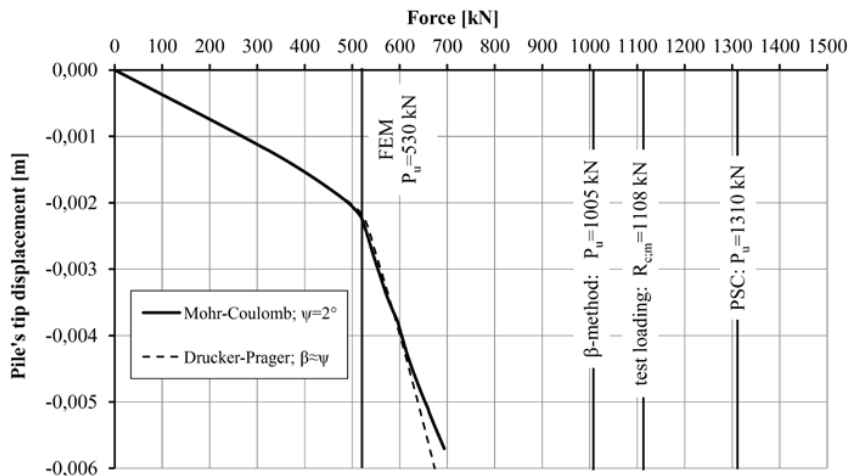

Fig. 5. Comparison of pile bearing capacity calculation results

5. Conclusions

The finite element analysis with simple constitutive models and parameters' estimation shows quite good agreement with the field test settlements for the loading part. Significant difference is seen for the unloading. Comparing curves for $\mu = \infty$ and tied nodes, one can see that the "elastic slip" related to contact formulation has some impact on results. For FEM analysis involving pile settlement the proper identification of the pile shaft-soil interface is of great importance. However, the real interface behavior is complicated and not fully understood. Elimination of the "elastic slip" for friction formulation involves using Lagrange multiplayers. It is not computationally efficient and the results presented herein show that it does not necessarily improve agreement with test data.

The FEA provides very safe estimation of bearing capacity. Often bearing capacity of piles is achieved at a displacement which is destructive for an engineering structure. Because of that, experience is needed in order to reduce bearing capacity values calculated assuming full mobilization of shaft friction.

Advanced soil constitutive models including Drucker-Prager/Cap, Cam/Clay, Hardening Soil and others should have been applied in order to perform sophisticated FEM simulations of bearing capacity problems. The differences in the pile bearing capacity estimation using various methods (Fig. 5) can be explained by the lack of detailed data characterizing soil layers. No hardening data was available though. Moreover, the moduli of elasticity used were estimated with very limited accuracy. Non-linear elasticity would have provided, probably, better agreement with load test results. However here, no bender element test results were available which could have provided data concerning small strain elastic moduli. Furthermore, during pile's construction process and later displacements, soil under the pile and around it can be compacted which changes granular soil's mechanical parameters. That could be implemented in a material model.

References

[1] T.W. Lambe, R.V. Whitman, Soil Mechanics, Wiley, New York, 1969,
[2] F. Oka, S. Kimoto, Computational modeling of Multiphase Geomaterials, CRC Press, New York, 2013,
[3] PN-83/B-02482, Foundations. Bearing capacity of piles and pile foundations., Polish Committee for Standardization, 1983,
[4] PN-EN 1997-1, Eurocode 7: Geotechnical design, Polish Committee for Standardization, 2008,
[5] Design documentation provided by the General Project Contractor STRABAG,
[6] Z. Wiłun, An outline geotechnics, WKŁ, Warsaw, 1987, (in Polish),
[7] Wei Dong Guo, Theory and Practice of Pile Foundations, CRC Press, New York, 2013,
[8] O. Puła, Pile foundations according to Eurocode 7, DWE, Wroclaw, 2013, (in Polish),
[9] F.H. Kuhlawy, Limiting tip and side resistance: Fact or fallacy? Analysis and design of pile foundations, ASCE Proc Geotech Eng Symp, 1984, pp. 80-98,
[10] L.C. Reese, M.W. O'Neill, New design method for drilled shaft from common soil and rock tests, ASCE Proc Foundation Engr Current Principles and Practices, 1989, pp. 1026-1039 ,
[11] B. McClelland, Design of Deep Penetration Piles for Ocean Structures, ASCE J. of Geotechnical Eng., 1974, pp. 705-747,
[12] H.-Y. Fang, Foundation Engineering handbook, Van Nostrand Reinhold, New York, 1991,
[13] V.G. Berezantzev, V.S. Khristoforv and V.N. Golubkov, Load-bearing capacity and deformation of piled foundations, Proc 5th Int Conf on Soil Mech and Found Eng, speciality session 10, Paris, 2:11-5 ,
[14] N. Janbu, ed., Static bearing capacity of friction piles, Proc of the 6th Europ Conf on Soil Mech and Found Eng., Vol. 1.2, 1976, pp. 479-488.